Functional Mapping of the Human Somatosensory Cortex with Echo-Planar MRI

Kuniyoshi Sakai, Eiju Watanabe, Yukari Onodera, Hiroyuki Itagaki, Etsuji Yamamoto, Hideaki Koizumi, Yasushi Miyashita

The somatotopical organization of the human somatosensory cortex was analyzed with echo-planar imaging at 1.5 Tesla, utilizing deoxyhemoglobin as an endogenous contrast medium. Scrubbing stimulation at a frequency of 3 Hz was applied to one of three cutaneous areas: toes, fingertips, and tongue tip. Parasagittal echo-planar slices were obtained every 2 s. We found focal bands of increased signal intensity (4% on average) during the stimulation, with a rise time of 2–6 s. These activated bands were located on the contralateral postcentral gyrus. The cortical responses from the three stimulation sites were anatomically distinct and organized medially-to-laterally in the order of toes, fingertips, and tongue tip.

Key words: functional MRI; echo-planar imaging; human brain mapping; somatosensory cortex.

INTRODUCTION

Recent development of the noninvasive techniques of functional magnetic resonance imaging (fMRI) has enabled human brain mapping without the need for an exogenous contrast medium (1, 2). It has been demonstrated that the underlying mechanism is a local change in magnetic susceptibility related to blood oxygenation level dependent signal (3), the elevation of which accompanies increased neuronal activity (4). One significant advancement of fMRI is the application of an ultra-fast echo-planar imaging (EPI) sequence (5), which improves temporal resolution and thus enables dynamic mapping (6, 7).

In order to estimate the spatial resolution of imaging techniques, it is useful to study topographical organization of sensory cortices. Positron emission tomography (PET) studies have already documented retinotopy (8) and somatotopy (9, 10), in which spatial resolution of scanning is typically more than 10 mm full width at half-maximum. Recently, retinotopy has been further characterized by fMRI studies with the resolution of 1–2 mm (11, 12). Using fMRI, we report here the characterization of somatotopy by applying appropriate tactile stimulation to distinct cutaneous areas in the primary somatosensory cortex (SI). The physiological assessment of the spatial resolution of fMRI has been hampered, because the contribution of venous vessels to changes of signal intensity remains controversial. We used a magnetic resonance angiography (MRA) scan to identify major veins and to exclude the possibility of their main contribution. As for the temporal resolution, we utilized the ultra-fast EPI sequence to measure the time course of signal changes. A part of this study has been reported in abstract form (13, 14).

METHODS

Functional magnetic resonance imaging experiments were performed by using a 1.5 T fMRI system equipped with EPI sequence, which was developed at Hitachi Central Research Laboratory. The gradient coils of elliptic cylinder shape (width, 52 cm; height, 40 cm; length, 50 cm) were designed to alleviate the power requirements for gradient field drivers. Their maximum strengths were G_x = 24 mT/m, G_y = 36 mT/m, G_z = 40 mT/m. The RF coil (quadrature coil) of cylinder shape (diameter, 26 cm; length, 20 cm) was optimized to enhance its sensitivity without degrading the local homogeneity of the RF field in cortical regions. An RF shield (diameter, 33 cm; length, 25 cm) surrounded this RF coil. Approval for these human experiments was obtained from the institutional review board of the University of Tokyo, School of Medicine.

Six normal right-handed volunteers aged 23–43 years were examined in this study. The subjects were in a supine position in the magnet, and their heads were held still with padding inside the RF coil. The subjects' eyes were closed, and the room lights were dimmed. Extraneous sounds were dampened with plastic molds placed in the ear canals. The scrubbing stimulation was applied manually at a frequency of 3 Hz, and the stimulation was synchronized with the sound of EPI beats (2-s interval). We tested three cutaneous areas: right toes, right (or left) fingertips of Digits 1–3, and tongue tip. Toes were stimulated from the tibial side to the peroneal side using a big brush (outer size, 7 × 9 cm^2; contact area of polypropylene filaments, 180 mm^2) with a 3-kg bending force and 17 g/mm^2 bending pressure. Fingertips were stimu-

MRM 33:736–743 (1995)

From the Department of Physiology, School of Medicine, University of Tokyo (K.S., Y.M.); Department of Neurosurgery, Tokyo Metropolitan Police Hospital (E.W.); and Central Research Laboratory, Hitachi, Ltd. (Y.O., H.I., E.Y., H.K.), Tokyo, Japan.

Address correspondence to: Kuniyoshi Sakai, Ph.D., MGH-NMR Center, Massachusetts General Hospital and Harvard Medical School, Building 149, 13th Street, Charlestown, MA 02129.

Received July 5, 1994; revised January 16, 1995; accepted January 16, 1995.

This work was supported by Grant-in-Aid for Specially Promoted Research from the Japanese Ministry of Education, Science and Culture (No. 02102008). K. S. was supported by a grant from Hayao Nakayama Foundation for Science & Technology and Culture.

0740-3194/95 $3.00

lated from the radial side to the ulnar side using a small brush (outer size, 1 × 2.5 cm^2; contact area of polybutylene terephthalate filaments, 70 mm^2) with a 1-kg bending force and 14 g/mm^2 bending pressure. Tongue tip was stimulated from the medial side to the right side (2-cm long) using a cotton swab (stick diameter, 2 mm) with a 30-g bending force and 10-g/mm^2 bending pressure. The scrubbing stimulus for each cutaneous area caused no pain, and the consistency of stimulus application was confirmed by the subject's report. These intensities of bending pressure were matched with a standard value of 16 g/mm^2 for receptive field mapping in the primate SI with the use of suprathreshold nylon monofilament von Frey hairs (15): von Frey filaments have been extensively used to assess touch-pressure sensation (16). We also tested vibrotactile stimulation on fingertips of Digits 1–4 at a frequency of 125 Hz and an amplitude of 2 mm, which are the same parameters as those in the PET studies (9, 10).

Each stimulation trial consists of the first resting period of 40 s (or 30 s), tactile stimulation period of 30 s, and the second resting period of 40 s. A single session consists of 7 to 16 trials. For the functional imaging, we utilized a blipped, gradient-echo EPI pulse sequence with a flip angle (FA) of 90° to give T_2* weighting that is sensitive to local deoxyhemoglobin levels. The data acquisition time was 60 ms/slice with the half Fourier method. Parasagittal EP slices of 1- or 1.5-cm thickness (field of view (FOV), 260 × 260 mm^2; in-plane resolution, 2 × 4 mm^2) were obtained every 2 s (*TR*) during each trial. The in-plane size of each pixel in an EP image was 2 × 2 mm^2 after linear interpolation. A spin-echo (SE) image with T_1 weighting (*TR* = 500 ms; *TE* = 30 ms) of the corresponding parasagittal slice (FOV, 260 × 260 mm^2; in-plane resolution, 1 × 1 mm^2) was taken every 7 or 8 trials. This SE image was utilized for the confirmation of the head position and for the anatomical registration of activated regions.

Each pixel in an EP image corresponds approximately to the pixel in the same position of an SE image, because the same field of view and slice parameters were used for the same gradient coils. The expected geometric distortion for EP images was calculated as follows. Because the signal was sampled at 370 kHz for an area of 520 × 260 mm^2 (readout × phase-encode), the bandwidth/pixel (pixel size, 2 × 2 mm^2) due to sampling characteristics for the readout direction (dorso-ventral axis) is

$$\Delta f/f_0 = 370\ \text{kHz}/(63.8\ \text{MHz} \times 128 \times 2) = 23\ \text{ppm}. \quad [1]$$

Assuming 0.2-ppm inhomogeneity across a pixel, the distortion in the readout direction is negligibly small (0.01 pixel). For the phase-encode direction (antero-posterior axis), the geometric distortion due to 0.1-ppm field inhomogeneity ΔB (0.15μT) can be estimated as

$$\Delta y = (\gamma/2\pi) \times \Delta B \times \tau \times \text{FOV} = 1.3\ \text{mm}, \quad [2]$$

in which γ is the gyromagnetic ratio of proton ($\gamma/2\pi$ = 42.6MHz/T), and τ is the interval of echos (0.8ms). Because the field inhomogeneity in the anatomical region is less than 0.2 ppm, the distortion in the phase-encode direction is less than 1 pixel. Moreover, we carefully adjusted the head position laterally and dorsally so that the post central gyrus to be observed was near the center of the magnet, where the spatial distortion was minimal.

Before EP scans in a single session, we first obtained the SE image of a coronal section for the same subject and selected a parasagittal plane to be observed. Next, we obtained the SE image of the parasagittal plane and identified the postcentral gyrus on this SE image. To estimate the mediolateral position of activated areas, we first adopted the multislicing technique for three adjacent EP slices (each thickness = 1 cm) and stimulated one cutaneous area. Then we determined the center of one parasagittal slice that would maximize the signal-to-noise ratio and acquired the final EPI data using this single slice position.

We identified areas with signal increase related to tactile stimulation by the following procedures. First, we averaged images in the first resting period of each trial and normalized all images of that trial with this averaged image for each voxel. The first five images at the sampling onset were excluded from averaging to ensure the stable resting condition of brain tissues as well as the subject's alertness. Next, we pooled normalized images in the first resting period of all trials in a single session as "OFF" data. For "ON" data, we pooled normalized images in the stimulation period of all trials in the same session except for the first three images in this period, which might reflect a transitional phase. Statistical significance of signal changes (ON versus OFF) was assessed with two-sided Student's *t*-test for each voxel. Voxels with insignificant and negative *t*-values were zero-filled, because negative correlations were not investigated in this study. These *t*-values were then superimposed on the corresponding anatomical SE image with a color scale. This color map is called here an activation *t*-map. Data processing was performed on HP375 and HP720 computers (Hewlett-Packard Company, Cupertino, CA) with custom software.

We also utilized a conventional MRI scanner, MRH-1500 (Hitachi Medical Corporation, Tokyo, Japan), for the MRA study to identify major veins. An MRA scan was run with a three-dimensional (3D) phase contrast sequence (17) (*TR* = 40 ms; *TE* = 17 ms; FA = 20°; flow for a phase shift of π, 10 cm/s; FOV, 220 × 220 mm^2; horizontal in-plane resolution, 0.86 × 0.86 mm^2; slice thickness, 2 mm; bulk thickness, 48 mm from the dorsal surface; with flow compensation; no presaturation; no contrast medium). This sequence permits the visualization of small vessels having relatively slow flow. For the surface structure imaging, a two-dimensional (2D) fast SE image with T_2 weighting was obtained (*TR* = 3000 ms; *TE* = 170 ms; FA = 90°; FOV, 220 × 220 mm^2; in-plane resolution, 0.86 × 0.86 mm^2; slice thickness, 50 mm). This sequence enhances surface cerebrospinal fluid with long T_2 relaxation time. Note that the surface structure image in Fig. 1 is shown black and white reversed. The overlay of an MRA image on a surface structure image was performed with ANALYZE software (Mayo Clinic and Foundation, Rochester, MN).

RESULTS

Reliable identification of the central sulcus was realized with the surface structure imaging of the dorsal cortex (Fig. 1). On this surface image, major vessels were visualized using an MRA technique. We observed that the location of superior cerebral veins varies considerably with each hemisphere. In the left hemisphere shown in Fig. 1, two thick veins were in the precentral sulcus and the postcentral sulcus. Much thinner veins were found in the vicinity of the superior sagittal sinus. Because there were no major veins in the central sulcus, we studied this subject most extensively. This method is particularly important, because it has been argued that changes of signal intensity might originate from superficial veins rather than the cortical parenchyma.

We found that the scrubbing stimulation on fingertips produced a significant increase of signal intensity in parasagittal slices approximately at the level of lateral 40 mm (the middle of the thickness of slices). Fig. 2a shows the activated areas localized within the contralateral postcentral gyrus at the level of lateral 42 mm (L 42). This region extended along the central sulcus as a band, and its in-plane size was 27 × 4 mm^2. This band did not correspond with the location of the MRA-imaged veins in the same subject (Fig. 1), which showed no significant activation. The upper end of the focal band in this slice (L 42) was located in the middle of the entire span of the central sulcus. The parasagittal slices that showed postcentral gyrus activation by fingertip stimulation were centered at L 40.0 ± 1.9 mm in one subject (Table 1), and this result was confirmed in other subjects (Table 2). We also confirmed that there was no comparable activation in the ipsilateral postcentral gyrus.

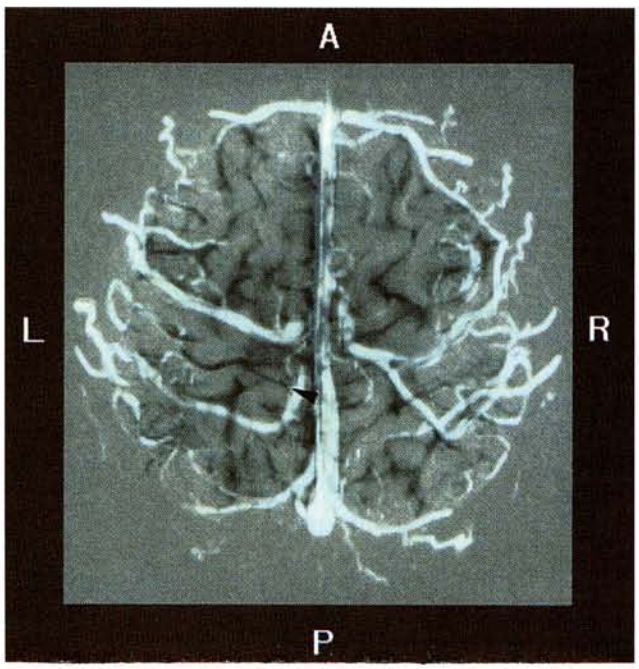

FIG. 1. The identification of the central sulcus and major venous vessels. An overlay of an MRA image on a surface structure image of the dorsal cortex (top view). Cerebral sulci and fissures are shown in black. A black arrowhead indicates the left central sulcus. The postcentral gyrus locates posteriorly to the central sulcus. The MRA image of vessels (shown in blue and white) was obtained with a maximum intensity projection through the dorsoventral axis. The vessel along the midline is the superior sagittal sinus. In the left hemisphere, major superior cerebral veins are located in the precentral sulcus and the postcentral sulcus, whereas other thinner veins can be found in the vicinity of the superior sagittal sinus. Note that there were no major veins in the central sulcus in the left hemisphere. A, anterior; P, posterior; L, left; R, right.

Table 1
Location and Intensity of Activation in the Postcentral Gyrus (Intrasubject)

Stimulated area (scrubbing)	Lateral location (mm)	Maximum intensity (%)	*t*-value	Degrees of freedom
R Fingertips	L 41	6.7	11.8	41
L Fingertips	R 39	6.4	4.7	41
R Fingertips	L 38	3.1	6.1	65
L Fingertips	R 42	5.5	6.8	64
R Fingertips	L 38	2.8	5.7	160
L Fingertips	R 42	2.3	9.1	159
R Fingertips	L 42	4.7	10.4	131
R Fingertips	L 38	2.1	9.1	106
mean ± SD	L 40.0 ± 1.9	4.2 ± 1.9		
Tongue tip	L 54	4.8	6.9	79
Tongue tip	L 56	4.7	12.5	160
Tongue tip	L 50	2.4	6.3	233
mean ± SD	L 53.3 ± 3.1	4.0 ± 1.4		
R Toes	L 7	5.1	13.0	106
R Toes	L 5	4.0	5.4	79
R Toes	L 5	3.5	9.1	106
R Toes	L 5	2.7	12.1	213
R Toes	L 5	6.8	9.6	106
mean ± SD	L 5.4 ± 0.9	4.4 ± 1.6		

R, right; L, left; SD, standard deviation. Each row corresponds to a single session for Subject 1. Lateral location is the lateral distance at the middle of the thickness of parasagittal slices. Maximum intensity is the percent change in MRI signal (averaged for all trials in a single session) for one voxel located in the postcentral gyrus. These data are highly significant as shown by large *t*-values.

Table 2
Location and Intensity of Activation in the Postcentral Gyrus (Intersubject)

Stimulated area (scrubbing)	Subject	Lateral location (mm)	Maximum intensity (%)
Fingertips	1	L 40.0	4.2
Fingertips	2	L 37.0	1.9
Fingertips	3	L 40.5	3.1
Fingertips	4	L 38.0	2.7
mean ± SD		L 38.9 ± 1.7	3.0 ± 1.0
Tongue tip	1	L 53.3	4.0
Tongue tip	2	L 53.0	6.7
Tongue tip	3	L 53.0	2.2
Tongue tip	5	L 54.0	5.2
mean ± SD		L 53.3 ± 0.5	4.5 ± 1.9
Toes	1	L 5.4	4.4
Toes	2	L 4.0	2.6
Toes	4	L 3.0	4.8
Toes	5	L 5.0	3.7
mean ± SD		L 4.4 ± 1.1	3.9 ± 1.0

L, lateral; SD, standard deviation. Each row corresponds to data averaged for each subject. Lateral location is the lateral distance at the middle of the thickness of parasagittal slices. Maximum intensity is the percent change in MRI signal for one voxel located in the postcentral gyrus.

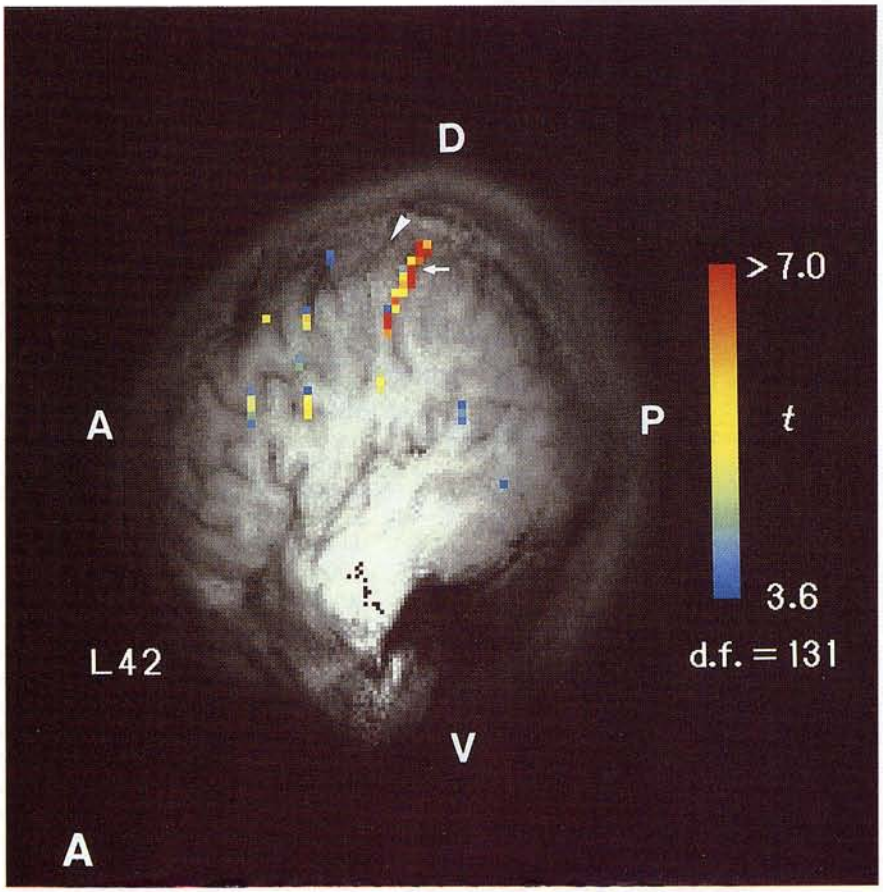

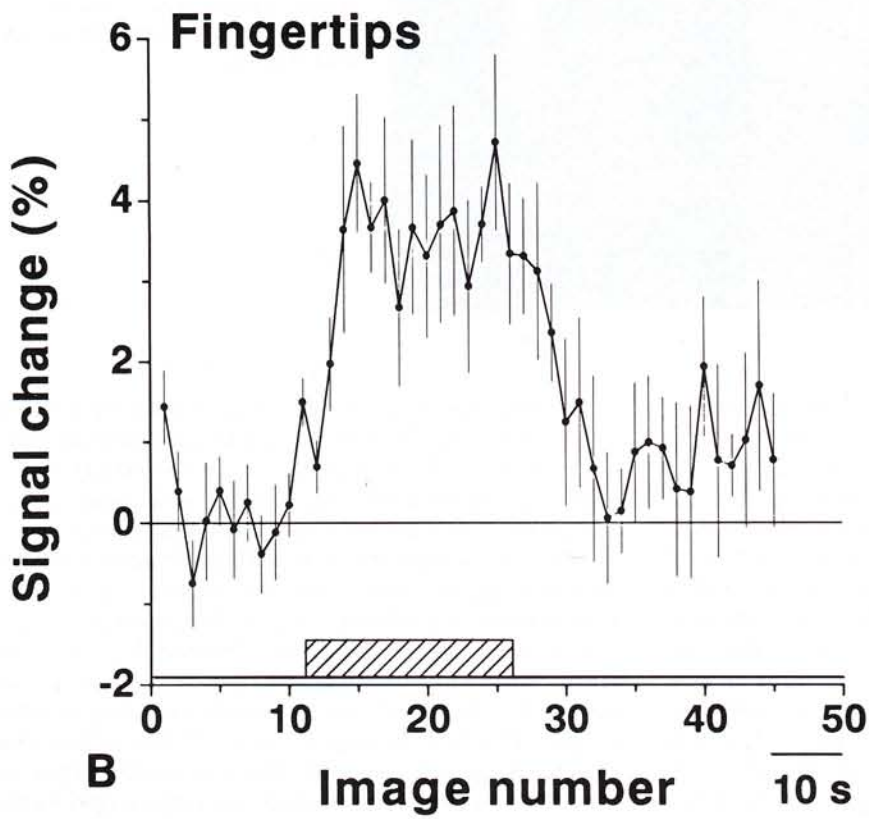

FIG. 2. Time-locked focal activation in the postcentral gyrus during fingertip stimulation. (a) The activation *t*-map of a left parasagittal slice centered at L 42 (thickness, 1.5 cm), for the same subject shown in Fig. 1. An arrowhead indicates the central sulcus. The color scale is linear in units of *t*-values and represents significance level of increased signal intensity. The colored voxels represent areas of highly significant change ($P < 0.001$) in signal intensity. Degrees of freedom (d.f.) are indicated, assuming that each image is an independent sample. This activation *t*-map shows the areas of signal increase induced by the scrubbing stimulation on right fingertips, in comparison to the resting condition. The activated band is clearly localized in the postcentral gyrus. A, anterior; P, posterior; D, dorsal; V, ventral. (b) The time course of the signal change at a single voxel in the postcentral gyrus. This typical voxel is indicated by an arrow in (a). The mean and standard error values ($n = 5$) are plotted against image number (2 s/image), in which *n* refers to the number of trials within a single session for one subject. The stimulation was applied from image No. 11 to image No. 26, as denoted by a hatched rectangle. Note the time-locked signal increase and recovery.

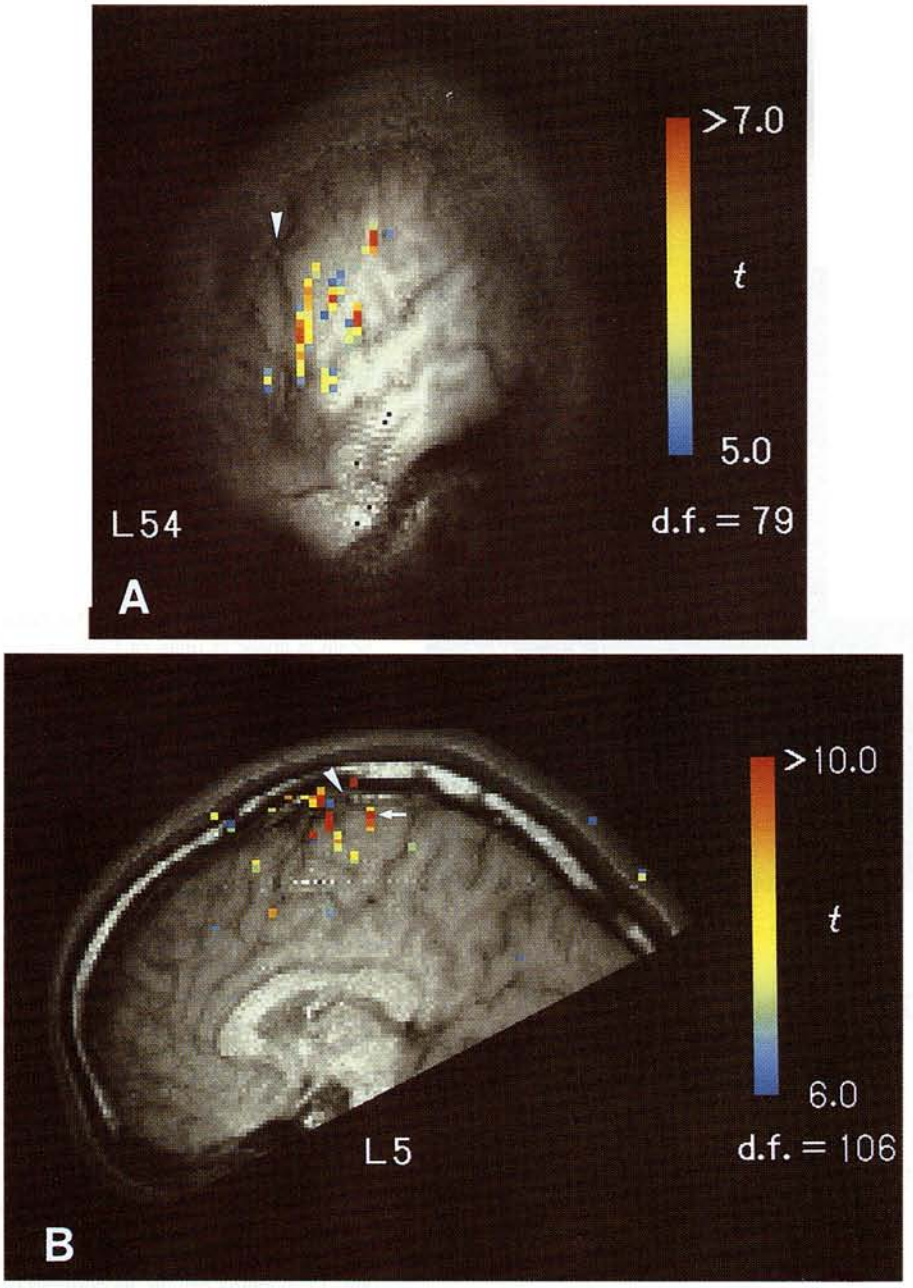

FIG. 3. Focal bands of activation in the postcentral gyrus during tongue tip and toe stimulation. (a) The activation *t*-map of a left parasagittal slice centered at L 54 (thickness, 1.5 cm). The orientation of the figure is the same as that of Fig. 2a. An arrowhead indicates the central sulcus. The colored voxels represent areas of highly significant change ($P < 0.001$) in signal intensity. Degrees of freedom (d.f.) are indicated, assuming that each image is an independent sample. This activation *t*-map shows the areas of signal increase induced by the scrubbing stimulation on the tongue tip, in comparison to the resting condition. One activated band is localized in the postcentral gyrus. (b) The activation *t*-map of a left sagittal slice centered at L 5 (thickness, 1.0 cm). The orientation of the figure is the same as that of Fig. 2a. An arrowhead indicates the central sulcus. This activation *t*-map shows the areas of signal increase induced by the scrubbing stimulation on the right toes, in comparison with the resting condition. One activated band is localized in the postcentral gyrus.

It has been shown that EPI is one of few techniques that can critically sample blood oxygenation level dependent contrast functional signal modulations. Fig. 2b demonstrates the signal change induced by fingertip stimulation. Just after applying the stimulation, the signal intensity increased and reached a plateau of about 4% level with a rise time of 2–6 s. The recovery time required to reach the resting level after termination of the stimulation was slightly longer than the rise time. This time course was reproducible in every trial as indicated by the value of standard error. In contrast to other techniques of electroencephalography and magnetoencephalography, the signal-to-noise ratio of fMRI is high enough to observe a stimulus-dependent time course, even in a single trial.

We then tested the effect of scrubbing on different cutaneous areas. Because the preferred stimulus varies significantly with cutaneous areas, we selected a cotton swab for the scrubbing (or tapping) stimulation of the tongue tip. The activated areas were found in a slice more lateral (Fig. 3a) than the slice for fingertip activation. The area showing the highest level of activation was the focal band within the postcentral gyrus. The parasagittal slices that showed postcentral gyrus activation by tongue tip stimulation were centered at L 53.3 ± 3.1 mm in one subject (Table 1), and this result was confirmed in other subjects (Table 2). More posteriorly, we found that other regions were activated with this stimulation. They included a portion of the parietal operculum (red voxels near the sylvian fissure in Fig. 3a), which has been sug-

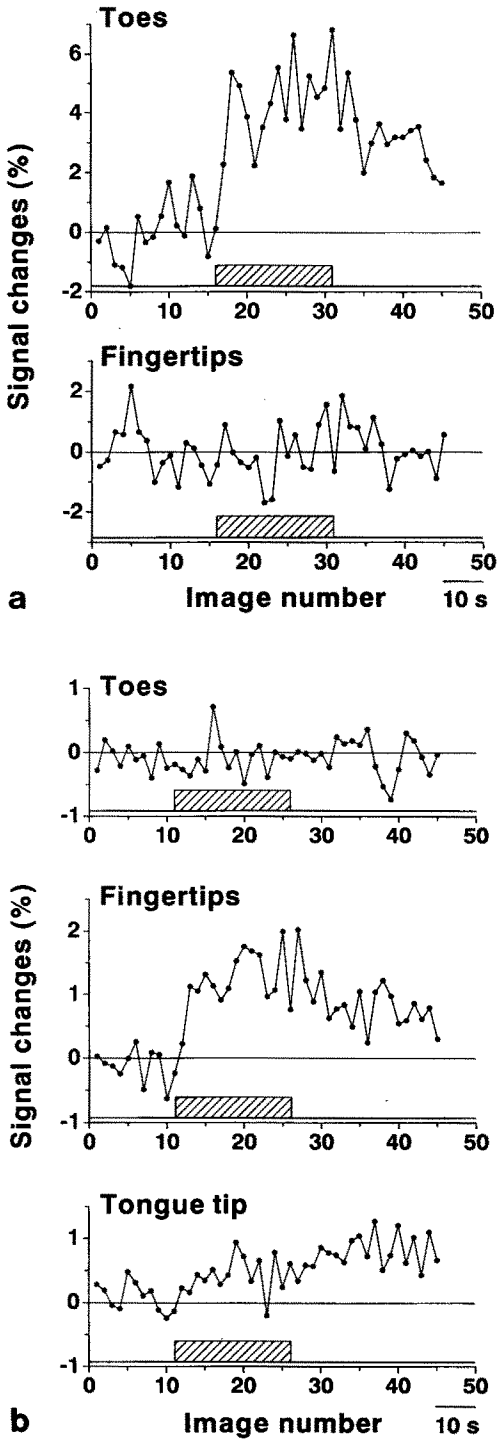

FIG. 4. Somatotopical organization revealed by the stimulus selectivity of the cortical activation. (a) The time course of the signal changes at a single voxel in the postcentral gyrus, observed in a left sagittal slice centered at L 5 (thickness, 1.0 cm). This typical voxel is indicated by an arrow in Fig. 3b. The mean values (n = 4) are plotted against image number (2 s/image), in which n refers to the number of trials within a single session for one subject. The stimulation was applied from image No. 16 to image No. 31, as denoted by hatched rectangles. Note the time-locked signal increase and recovery that are induced by the stimulation of right toes (upper), but not by the stimulation of right fingertips (lower). (b) The time course of the signal changes at a single voxel in the postcentral gyrus, observed in a left parasagittal slice centered at L 38 (thickness, 1.5 cm). The mean values (n = 4) are plotted against image number (2 s/image). The stimulation was applied from image No. 11 to image No. 26, as denoted by hatched rectangles. Note the time-locked signal increase and recovery that are induced by the stimulation of right fingertips (middle), but not by the stimulation of right toes (upper) or tongue tip (lower).

gested as the secondary somatosensory area (see ref. 10 for a recent PET study on the secondary somatosensory area).

We further tested the scrubbing stimulation on toes, using a bigger and harder brush than the brush for fingertip stimulation. The activated areas were found in a medial sagittal slice centered approximately at L 5 (Fig. 3b). The area showing the highest level of activation was within the postcentral gyrus, which is anterior to the cingulate sulcus (pars marginalis). The parasagittal slices that showed postcentral gyrus activation by toe stimulation were centered at L 5.4 ± 0.9 mm in one subject (Table 1), and this result was confirmed in other subjects (Table 2). Other activated regions were in the precentral gyrus, which might suggest the feedback of sensory input to the primary motor cortex or the isometric contraction of foot muscles in resisting the stimulus force.

As shown in Tables 1 and 2, the lateral locations of activation that correspond to the three stimulation sites were significantly different for intrasubject comparison ($P < 0.0001$, $F(2, 8) = 735$; F test with unequal variances (18)) and for intersubject comparison ($P < 0.0001$, $F(2, 5) = 1850$). The locations for fingertips and tongue tip were significantly different for intrasubject comparison ($P < 0.01$, $t'(3) = 6.96$; t test with unequal variances (18)) and for intersubject comparison ($P < 0.001$, $t'(4) = 16.25$), and the difference between the location of fingertips or tongue tip and that of toes was unequivocally significant. These results clearly confirm the somatotopy in the human somatosensory cortex. On the other hand, there was no significant difference in the maximum intensities of activation induced by the three stimuli for intrasubject comparison ($P > 0.1$, $F(2, 12) = 0.068$) as well as for intersubject comparison ($P > 0.1$, $F(2, 6) = 1.33$), which confirms that these stimuli were equally effective.

A more direct demonstration of somatotopical organization is the stimulus selectivity of the cortical activation. We tested toe stimulation and fingertip stimulation alternately in different trials of a single session. The time course of signal changes at a single voxel in the postcentral gyrus showed distinct stimulus selectivity. Within sagittal slices centered approximately at L 5, there was a time-locked signal increase with toe stimulation but not with fingertip stimulation (Fig. 4a). This observation was further confirmed in more lateral parasagittal slices, with testing of all three kinds of stimulation. Both the time-locked signal increase and recovery were found only for fingertip stimulation; neither toe stimulation nor tongue tip stimulation induced a comparable effect (Fig. 4b).

Previous PET studies reported the activation of the somatosensory cortex by vibrotactile stimulation (9, 10). We confirmed this observation using the same parameters of stimulation (13). We tested two subjects and results were reproducible within one subject (the 6th sub-

ject). As to the vibrotactile stimulation on fingertips, the activated areas were localized within the postcentral gyrus at the level of L 39.1 ± 2.0 mm (N = 8 within this subject). This lateral level of the parasagittal slices matched with that for the scrubbing stimulation on fingertips (mean, L 38.9 in Table 2). Because the other subject (Subject 1 in Table 1) did not show consistent activation, we tested scrubbing stimulation instead and found reproducible activation within and across subjects.

DISCUSSION

We found that the focal bands induced by stimulation of the three cutaneous areas were organized medially-to-laterally in the order of toes (mean, L 4.4 in Table 2), fingertips (L 38.9), and tongue tip (L 53.3). Not only this order, but also the mediolateral positions agree well with the previous studies of the human somatosensory cortex with electrical stimulation (19), evoked potential recording (20), PET (9), and magnetoencephalography (21). Our study provides, to our knowledge, the first successful application of fMRI to somatotopical mapping. It requires higher spatial resolution than was achieved in this study to obtain a more detailed map for the somatotopical organization.

The rise time of 2–6 s found in this study is comparable to the delay time of signal increase in the human visual cortex observed with fMRI, utilizing a flashing checkerboard pattern at 8 Hz as a visual stimulus (7). Moreover, the similar rise time revealed by optical imaging of intrinsic signals (activity-dependent absorption at 630 nm) (22) indicates that the same mechanisms might be involved. In contrast to the rise time, the recovery time required to reach the resting level was found to be more variable (Figs. 2b, 4a, and 4b). The recovery time might depend on several factors: the stimulus modality (e.g., scrubbing or vibration), the stimulus site (fingertips, etc.), and the stimulus duration (here, 30 s). It would be interesting to study whether the recovery time correlates with the duration of after-sensation.

A recent study of motor responses showed that a pial vein in the central sulcus matched with the region in which signal changes were induced by finger motion (23). Because of the following reasons, it is unlikely that the focal bands induced by tactile stimulation were due to signals entirely from a single vein in the central sulcus. First, there were no major vessels in either the central sulcus or the postcentral gyrus (Fig. 1). Second, the activated band in Fig. 2a is localized within the postcentral gyrus, and it is at least 4 mm from the central sulcus. Third, we observed the stimulus-selective signal changes in the focal bands (Fig. 4), demonstrating the existence of distinct bands activated by the stimulation of single cutaneous areas. It suggests that these bands correspond to a limited range of topographically organized areas. Although it remains to be studied whether the origin of the signal is the cortical parenchyma, our present study clearly demonstrates that the spatial resolution of fMRI is sufficient to reveal the somatotopy with physical tactile stimulation. This imaging technique shows promise for future dynamic mapping of activation in cognitive processes without physical stimulation (24).

ACKNOWLEDGMENTS

The authors thank Dr. Marcus E. Raichle for helpful discussion, and Mr. A. Takane and Ms. M. Sasajima from Hitachi Medical Corporation for their technical assistance.

REFERENCES

1. K. K. Kwong, J. W. Belliveau, D. A. Chesler, I. E. Goldberg, R. M. Weisskoff, B. P. Poncelet, D. N. Kennedy, B. E. Hoppel, M. S. Cohen, R. Turner, H.-M. Cheng, T. J. Brady, B. R. Rosen, Dynamic magnetic resonance imaging of human brain activity during primary sensory stimulation. *Proc. Natl. Acad. Sci. (USA)* **89,** 5675–5679 (1992).
2. S. Ogawa, D. W. Tank, R. Menon, J. M. Ellermann, S.-G. Kim, H. Merkle, K. Ugurbil, Intrinsic signal changes accompanying sensory stimulation: functional brain mapping with magnetic resonance imaging. *Proc. Natl. Acad. Sci. (USA)* **89,** 5951–5955 (1992).
3. S. Ogawa, T. M. Lee, A. S. Nayak, P. Glynn, Oxygenation-sensitive contrast in magnetic resonance image of rodent brain at high magnetic fields. *Magn. Reson. Med.* **14,** 68–78 (1990).
4. P. T. Fox, M. E. Raichle, Focal physiological uncoupling of cerebral blood flow and oxidative metabolism during somatosensory stimulation in human subjects. *Proc. Natl. Acad. Sci. (USA)* **83,** 1140–1144 (1986).
5. M. K. Stehling, R. Turner, P. Mansfield, Echo-planar imaging: magnetic resonance imaging in a fraction of a second. *Science (Washington, DC)* **254,** 43–50 (1991).
6. P. A. Bandettini, E. C. Wong, R. S. Hinks, R. S. Tikofsky, J. S. Hyde, Time course EPI of human brain function during task activation. *Magn. Reson. Med.* **25,** 390–397 (1992).
7. A. M. Blamire, S. Ogawa, K. Ugurbil, D. Rothman, G. McCarthy, J. M. Ellermann, F. Hyder, Z. Rattner, G. L. Shulman, Dynamic mapping of the human visual cortex by high-speed magnetic resonance imaging. *Proc. Natl. Acad. Sci. (USA)* **89,** 11069–11073 (1992).
8. P. T. Fox, F. M. Miezin, J. M. Allman, R. Vogels, M. E. Raichle, Retinotopic organization of human visual cortex mapped with positron-emission tomography. *J. Neurosci.* **7,** 913–922 (1987).
9. P. T. Fox, H. Burton, M. E. Raichle, Mapping human somatosensory cortex with positron emission tomography. *J. Neurosurg.* **67,** 34–43 (1987).
10. H. Burton, T. O. Videen, M. E. Raichle, Tactile- vibration-activated foci in insular and parietal-opercular cortex studied with positron emission tomography: mapping the second somatosensory area in humans. *Somatosens. Mot. Res.* **10,** 297–308 (1993).
11. W. Schneider, D. C. Noll, J. D. Cohen, Functional topographic mapping of the cortical ribbon in human vision with conventional MRI scanners. *Nature (Lond.)* **365,** 150–153 (1993).
12. S. A. Engel, D. E. Rumelhart, B. A. Wandell, A. T. Lee, G. H. Glover, E.-J. Chichilnisky, M. N. Shadlen, fMRI of human visual cortex. *Nature (Lond.)* **369,** 525 (1994).
13. K. Sakai, E. Watanabe, Y. Onodera, H. Itagaki, E. Yamamoto, H. Koizumi, Y. Miyashita, Noninvasive functional mapping of human somatosensory cortex with echo planar magnetic resonance imaging. *Neurosci. Res.* **Suppl. 18,** S200 (1993).
14. K. Sakai, E. Watanabe, Y. Onodera, H. Itagaki, E. Yamamoto, H. Koizumi, Y. Miyashita, Functional mapping of human somatosensory cortex with echo planar magnetic resonance

imaging. *Soc. Neurosci. Abstr.* **20,** 1386 (1994).
15. W. M. Jenkins, M. M. Merzenich, M. T. Ochs, T. Allard, E. Guíc-Robles, Functional reorganization of primary somatosensory cortex in adult owl monkeys after behaviorally controlled tactile stimulation. *J. Neurophysiol.* **63,** 82–104 (1990).
16. Quantitative sensory testing: a consensus report from the Peripheral Neuropathy Association. *Neurology* **43,** 1050–1052 (1993).
17. C. L. Dumoulin, S. P. Souza, M. F. Walker, W. Wagle, Three-dimensional phase contrast angiography. *Magn. Reson. Med.* **9,** 139–149 (1989).
18. G. W. Snedecor, W. G. Cochran, "Statistical Methods," Iowa State University Press, Ames, Iowa, 1989.
19. W. Penfield, E. Boldrey, Somatic motor and sensory representation in the cerebral cortex of man as studied by electrical stimulation. *Brain* **60,** 389–443 (1937).
20. C. N. Woolsey, T. C. Erickson, W. E. Gilson, Localization in somatic sensory and motor areas of human cerebral cortex as determined by direct recording of evoked potentials and electrical stimulation. *J. Neurosurg.* **51,** 476–506 (1979).
21. T. T. Yang, C. C. Gallen, B. J. Schwartz, F. E. Bloom, Noninvasive somatosensory homunculus mapping in humans by using a large-array biomagnetometer. *Proc. Natl. Acad. Sci. (USA)* **90,** 3098–3102 (1993).
22. A. Grinvald, R. D. Frostig, R. M. Siegel, E. Bartfeld, High-resolution optical imaging of functional brain architecture in the awake monkey. *Proc. Natl. Acad. Sci. (USA)* **88,** 11559–11563 (1991).
23. S. Lai, A. L. Hopkins, E. M. Haacke, D. Li, B. A. Wasserman, P. Buckley, L. Friedman, H. Meltzer, P. Hedera, R. Fiedland, Identification of vascular structures as a major source of signal contrast in high resolution 2D and 3D functional activation imaging of the motor cortex at 1.5T: preliminary results. *Magn. Reson. Med.* **30,** 387–392 (1993).
24. K. Sakai, Y. Miyashita, Visual imagery: an interaction between memory retrieval and focal attention. *Trends Neurosci.* **17,** 287–289 (1994).